Eur. Phys. J. C 12, 263–269 (2000)
Digital Object Identifier (DOI) 10.1007/s100529900155

THE EUROPEAN
PHYSICAL JOURNAL C

Solar magnetohydrodynamic modes and parametric resonance in neutrino spin–flavor conversion

N. Reggiani[1], M.M. Guzzo[2], J.H. Colonia[2], P.C. de Holanda[2,3]

[1] Instituto de Ciências Exatas, Pontifícia Universidade Católica de Campinas, 13020-970 Campinas, SP, Brazil
[2] Instituto de Física Gleb Wataghin, Universidade Estadual de Campinas - UNICAMP, 13083-970 Campinas, São Paulo, Brazil
[3] Instituto de Física Corpuscular, Universitat de València, 46100 Burjassot, València, Spain

Received: 4 March 1999 / Published online: 8 December 1999

Abstract. Consequences of parametric resonances on neutrino resonant spin–flavor precession (RSFP) arising from global magnetohydrodynamic waves in the Sun are investigated. We show that for typical magnetic field profiles which generate an RSFP solution to the solar neutrino anomaly, the effects of the parametric resonance can be found for neutrinos of which the energy is of order 0.1 to 1 MeV. This opens the possibility of investigating these effects using real time experiments, like Borexino or Hellaz.

1 Introduction

Nuclear reactions existing in the central part of the Sun produce left-handed electron neutrinos [1–4], which travel through a possibly large magnetic field before leaving the solar interior. Assuming a non-vanishing neutrino magnetic moment [5], neutrinos interacting with this field can be resonantly converted into sterile non-electron neutrinos or active non-electron antineutrinos, depending on them being Dirac or Majorana type, respectively. On the other extremity of the neutrino trajectory to the Earth, solar neutrino detectors [6–10] are mainly sensitive to left-handed electron neutrinos. Therefore, the measured flux of solar neutrinos after this possible interaction with the solar magnetic field is smaller than what is expected from the standard solar model calculation [1–4], which predicts no conversion of the original left-handed neutrinos. This mechanism, which is called resonant spin–flavor precession (RSFP), may be responsible for the experimentally observed solar neutrino deficit [6–10].

In recent analyses [11,12] it was argued that solar neutrino observations have to be sensitive to the effects of magnetohydrodynamic (MHD) fluctuations in the Sun if the resonant spin–flavor precession (RSFP) mechanism is the solution to the solar neutrino problem. This can be easily understood. The solar neutrino survival probability based on the RSFP mechanism crucially depends on the values of four independent quantities. Two of these are related to the neutrino properties: its magnetic moment μ_ν and the squared mass difference of the physical eigenstates involved in the conversion mechanism divided by their energy, $\Delta m/E$. The other two quantities are related to the physical environment in which neutrinos are inserted: the magnetic field profile $B(r)$ and the electron (and neutron, for Majorana neutrinos) number density distribution $N(r)$ along the neutrino trajectory. MHD affects the magnetic field profile as well as the matter density, and therefore its effects will strongly influence the RSFP neutrino survival probability. Indeed we believe that such consequences can be thought of as a test to this solution to the solar neutrino problem based on the RSFP mechanism [11,12].

We have recently considered the influence of the continuous region of the MHD spectrum on the neutrino RSFP phenomenon. This part of the spectrum introduces very localized fluctuations on the magnetic field [11] as well as in the matter density profile [12]. In the present paper we analyze the complementary portion of the MHD spectrum, i.e., the out-of-continuum spectrum, which generates global waves. These global waves extend over a large region of the neutrino trajectory inside the Sun and generate both magnetic and matter density fluctuations. They also are associated with a typical perturbation wavelength, $L_{\rm MHD}$ which has to be compared with the neutrino oscillation length L_m. In case that $L_{\rm MHD} << L_m$, the neutrino evolution is governed by the average magnetic field and matter density and the MHD fluctuations are unimportant. If $L_{\rm MHD} >> L_m$, the transition is adiabatic and the neutrino evolves following the magnetic and density change. Nevertheless, a very interesting process occurs when $L_{\rm MHD}$ is of the same order as L_m. In this case the influence of the fluctuations on neutrino conversion becomes appreciable. In the extreme case where $L_{\rm MHD} = L_m$, a parametric resonance [13] occurs maximizing the effect of the MHD fluctuations. We argue that the appearance of such a parametric resonance is quite likely in the Sun due to MHD fluctuations.

We found perturbations in the matter density and in the magnetic field which fluctuate with a period of the order of a few days, and with a fluctuation scale of $L_{\rm MHD} \approx 10^{-3}$–$10^{-2} \times R_\odot$, where $R_\odot$ is the solar radius. These are of the order of magnitude of the oscillation length of neutrinos under the RSFP mechanism, with suitable parameters to solve the solar neutrino anomaly.

We analyzed the fluctuation in the probability generated by these perturbations and found that for large regions of the solar neutrino spectrum this fluctuation can typically reach 10% of the sign due to parametric resonance, and could achieve 50% for specific values of the neutrino energy for some field configurations. This could be detected by appropriate real time detectors.

2 MHD modes and neutrino spin–flavor conversion

If we consider a non-vanishing neutrino magnetic moment, the interaction of such neutrinos with this magnetic field will generate neutrino spin–flavor conversion which is given by the evolution equations [5]

$$\mathrm{i}\frac{\mathrm{d}}{\mathrm{d}r}\begin{pmatrix}\nu_{\mathrm{R}}\\ \nu_{\mathrm{L}}\end{pmatrix} = \begin{pmatrix} -\frac{\sqrt{2}}{2}G_{\mathrm{F}}N_{\mathrm{eff.}}(r)+\frac{\Delta m}{4E} & \mu_\nu|\mathbf{B}_\perp(r)| \\ \mu_\nu|\mathbf{B}_\perp(r)| & \frac{\sqrt{2}}{2}G_{\mathrm{F}}N_{\mathrm{eff.}}(r)-\frac{\Delta m}{4E}\end{pmatrix} \times \begin{pmatrix}\nu_{\mathrm{R}}\\ \nu_{\mathrm{L}}\end{pmatrix}, \tag{1}$$

where ν_{L} (ν_{R}) is the left- (right-) handed component of the neutrino field, Δm is the squared mass difference of the corresponding physical fields, E is the neutrino energy, G_{F} is the Fermi constant, μ_ν is the neutrino magnetic moment and $|\mathbf{B}_\perp(r)|$ is the transverse component of the perturbed magnetic field. Finally, we have $N_{\mathrm{eff.}} = N_e(r) - N_n(r)$ for Majorana neutrinos, where $N_e(r)$ ($N_n(r)$) is the electron (neutron) number density distribution, in which case the final right-handed states ν_{R} are active non-electron antineutrinos. For Dirac neutrinos, $N_{\mathrm{eff.}} = N_e(r) -(1/2)N_n(r)$; in this case the right-handed final states are sterile non-electron neutrinos [5]. In this paper we will assume Majorana neutrinos. Note, however, that since $N_n \sim (1/6)N_e$ in all points inside the Sun, the difference of taking Dirac or Majorana neutrinos leads to a multiplicative factor of $\sim 10/11$, and does not lead to sensible alterations in our conclusions, which are, in this way, valid for Majorana or Dirac neutrinos.

MHD waves and instabilities generated by MHD theory [14] can alter the neutrino evolution since they can induce time fluctuations of the transverse component of the magnetic field $|\mathbf{B}_\perp(r)|$ as well as the matter density $N_e(r)$ appearing in (1). Such magnetic fluctuations are obtained assuming that they are generated by small displacements of the solar plasma ξ described by the linearized MHD equations [15].

We consider a cylinder involving the solar equatorial plane in such a way that the plane of the solar equator coincides with one of the planes of this cylinder perpendicular to the z axis, and we take the cylinder height approximately 0.01 to 0.1 $R_\odot$ (where $R_\odot \approx 6.96 \times 10^{10}$ cm is the solar radius). We also assume periodicity in the coordinate z which means that the matter density, pressure and magnetic field are considered equal towards the North and South directions from the solar equator plane, which is a good approximation if we are close to the equatorial plane. This leads to the conclusion that one should only solve the differential equation [16]

$$\frac{\mathrm{d}}{\mathrm{d}r}\left[f(r)\frac{\mathrm{d}}{\mathrm{d}r}(r\xi_r)\right] + h(r)(\xi_r) = 0, \tag{2}$$

where

$$f(r) = \frac{\gamma p + B_0^2}{r}\frac{(w^2-w_A^2)(w^2-w_S^2)}{(w^2-w_1^2)(w^2-w_2^2)}, \tag{3}$$

$$\begin{aligned} h(r) = {} & \rho_0\omega^2 - k^2B_0^2 + g\frac{\partial\rho_0}{\partial r} \\ & -\frac{1}{D}g\rho_0^2(\omega^2\rho_0 - k^2B_0^2)\left[gH + \frac{\omega^2}{r}\right] \\ & -\frac{\partial}{\partial r}\left[\frac{1}{D}\omega^2\rho_0^2 g(\omega^2\rho_0 - k^2B_0^2)\right] \end{aligned} \tag{4}$$

and

$$w_A^2 = \frac{k^2B_0^2}{\rho_0}, \quad w_S^2 = \frac{\gamma p}{\gamma p + B_0^2}\frac{k^2B_0^2}{\rho_0}, \tag{5}$$

$$w_{1,2}^2 = \frac{H(\gamma p + B_0^2)}{2\rho_0}\left\{1 \pm \left[1 - 4\frac{\gamma p k^2 B_0^2}{(\gamma p + B_0^2)^2 H}\right]^{1/2}\right\}, \tag{6}$$

$$D = \rho_0^2\omega^4 - H\left[\rho_0\omega^2(\gamma p + B_0^2) - \gamma p k^2 B_0^2\right], \tag{7}$$

$$H = \frac{m^2}{r^2} + k^2. \tag{8}$$

where $\mathbf{g}$ is the acceleration due to gravity, p is the pressure, $\gamma = C_p/C_v$ is the ratio of the specific heats, ρ_0 is the equilibrium matter density profile and $\mathbf{B}_0$ is the magnetic equilibrium profile in the Sun. Note that in the derivation of the above equations we considered the equilibrium magnetic profile B_0 in the z direction.

The Hain–Lüst equation shows singularities when $f(r) = 0$, that is, when $w^2 = w_A^2$ or $w^2 = w_S^2$, which regions in the w^2 parameter space are called Alfvén and slow continua, respectively. In the interval $0 \le r \le 1$ the functions w_A^2 and w_S^2 take continuous values that define the ranges of the values of w^2 that correspond to improper eigenvalues. Eigenvalues of the Hain–Lüst equation must be searched, therefore, outside the regions where $w^2 = w_A^2$ and $w^2 = w_S^2$, and they define the global modes which are associated with magnetic and density waves along the whole radius of the Sun.

3 Resolution of the Hain–Lüst and evolution equations

We calculated the MHD magnetic spectrum and its consequences for the solar neutrino propagation assuming certain values for the profiles of the solar matter density, the pressure, the magnetic field and for the magnetic moment.

3.1 Solar matter density distribution and pressure profile

For the solar matter density distribution ρ_0, and for the pressure p, we considered the standard solar model prediction, i.e., approximately monotonically decreasing exponential functions in the radial direction from the center to the surface of the Sun [1]. The density profile was used to calculate the acceleration of gravity.

As the density profile found in [1] is given just up to $r = 0.95$ we have performed our calculations just up to this value of r. The conditions that we imposed on ξ are over all calculated values of r: $0 < r < 0.95$.

3.2 Magnetic field profile

The global modes obtained with the magnetic fields used in the analysis of the effect of localized waves [11,12] are very similar to each other. So, we present the effect of these modes on the neutrino RSFP phenomenon for just one of these magnetic fields; one that we consider a good representative of the others:

$$B_0 = B_0(r) = \begin{cases} 1 \times 10^6 \left(\frac{0.2}{r+0.2}\right)^2 \text{ G for } & 0 < r \leq r_{\text{convec}}, \\ B_C(r) & \text{for } \; r > r_{\text{convec}}, \end{cases} \tag{9}$$

where B_C is the magnetic field in the convective zone given by the following profiles:

$$B_C^{\mathrm{I}}(r) = 4.88 \times 10^4 \left[1 - \left(\frac{r-0.7}{0.3}\right)^n\right] \text{ G} \quad \text{for } r > r_{\text{convec}}, \tag{10}$$

with $n = 6$ and $r_{\text{convec}} = 0.7$. This profile was used by Akhmedov, Lanza and Petcov [17] to show the consistence of the solar neutrino data with the RSFP phenomenon.

In order to illustrate the effect of the parametric resonance, we used other magnetic fields that have been used by different authors to solve the solar neutrino problem through the RSFP mechanism [18]:

$$B_C^{\mathrm{II}}(r) = \begin{cases} B_{\text{initial}} + [\frac{B_{\max} - B_{\text{initial}}}{r_{\max} - r_{\text{convec}}}](r - r_{\text{convec}}) \\ \quad \text{for } r_{\text{convec}} < r < r_{\max}, \\ \\ B_{\max} + [\frac{B_{\max} - B_{\text{final}}}{r_{\max} - 1.0}](r - r_{\max}) \\ \quad \text{for } r > r_{\max}, \end{cases} \tag{11}$$

where $B_{\text{initial}} = 2.75 \times 10^5$ G, $B_{\max} = 1.18 \times 10^6$ G, $B_{\text{final}} = 100$ G, $r_{\text{convec}} = 0.65$ and $r_{\max} = 0.8$. Although the magnetic field in this configuration seems to be too strong to be present in the convective layer of the Sun, we extend our analysis for this configuration because it is very useful to illustrate the parametric resonance effect for different values of the perturbation oscillation length. It is also important to notice that the important quantity for the neutrino evolution is not the magnetic field itself, but the product $\mu_\nu |\mathbf{B}_\perp(r)|$, which we pose to be of the same magnitude in the Sun convective layer for all magnetic field configuration chosen here, as we discuss in Sect. 3.5.

We considered also a third field, constant all over r, given by [19]

$$B_0 = 253\,\text{kG} \quad \text{for } 0 < r < 1.0. \tag{12}$$

We assume that the magnetic equilibrium profile B_0 is in the z direction.

3.3 Constraints on ρ_1 and b_1

To impose physical conditions on the solutions found for the Hain–Lüst equation, we calculated the perturbation of the density and of the magnetic field provoked by ξ, given by the equations

$$\mathbf{b}_1 = \nabla \times (\xi \times \mathbf{B}_0) \tag{13}$$

and

$$\rho_1 = \nabla \cdot (\rho \xi). \tag{14}$$

The matter density fluctuations are very constrained by helioseismology observations. The largest density fluctuations ρ_1 inside the Sun are induced by temperature fluctuations δT due to convection of matter between layers with different local temperatures. An estimate of such an effect is presented in [20] and gives

$$\frac{\rho_1}{\rho_0} = m_p g(r - r_0) \frac{\delta T}{T^2} = \frac{r - r_0}{R_0} \frac{\delta T}{T}, \tag{15}$$

where m_p is the nucleon mass, $g(r)$ is the acceleration of gravity and $R_0 \approx 0.09 \times R_\odot$ ($R_\odot$ is the solar radius) is a numerical factor coming from the approximately exponentially decreasing standard matter density distribution inside the Sun [1]. Since $(\langle \delta T^2 \rangle)^{1/2}/T \approx 0.05$ is not in conflict with helioseismology observations [21], taking $(r - r_0)/R_0 \approx 1$, we assume density fluctuations ρ_1/ρ_0 smaller than 10%. In fact, in an accurate analysis of the consequences of helioseismology for matter density fluctuations [22] it was concluded that ρ_1/ρ_0 can be very large (larger than 10%) only for the very inner parts of the Sun ($r < 0.04$) as well as for very superficial regions ($r > 0.98$). For $0.04 < r < 0.25$, ρ_1/ρ_0 decreases approximately linearly and achieves its smaller value, 2%, in $r \approx 0.25$. Finally, in the region where $0.4 < r < 0.9$, ρ_1/ρ_0 is approximately 5%. We impose these constraints as boundary conditions for the amplitudes of the density fluctuations we will consider later.

The size of the amplitude factor b_1 is not very constrained by the solar hydrostatic equilibrium, since the magnetic pressure $B_0^2/8\pi$ is negligibly small when compared with the dominant gas pressure if we consider the matter density distribution ρ_0 as predicted by the standard solar model and the magnetic field strength of order of the ones required to solve the solar neutrino anomaly

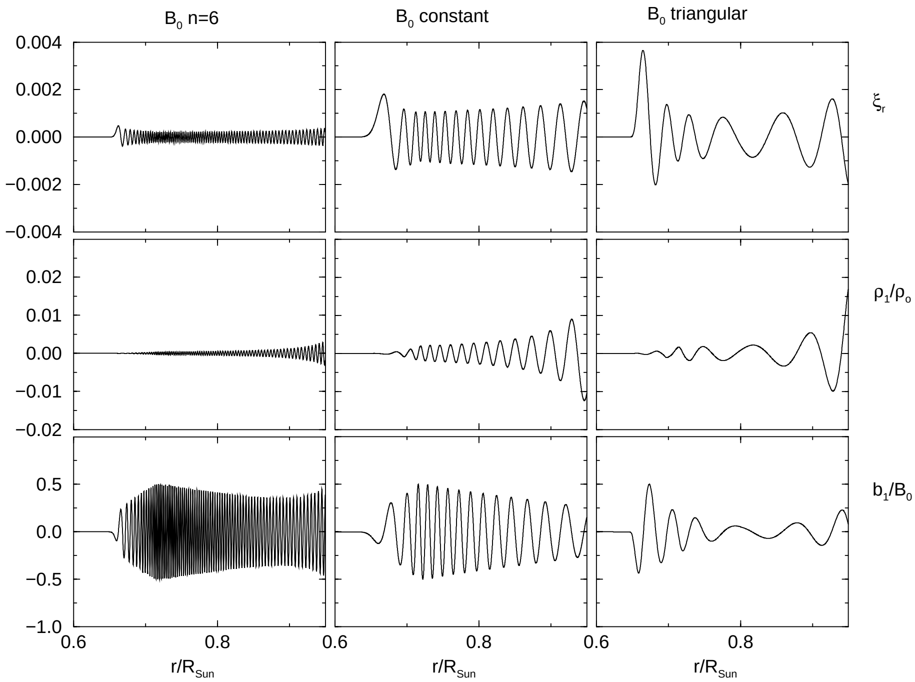

Fig. 1. Profile of **a** ξ_r, after normalization, **b** ρ_1/ρ_0 and **c** b_1/B_0; these are caused by the magnetohydrodynamic effect for the magnetic profiles given by (9) and (10) (B_0 $n=6$), (12) (B_0 constant) and (9) and (11) (B_0 triangular)

[17]. Despite this fact, it cannot be arbitrarily large when we are solving the Hain–Lüst equation. This equation is obtained after linearization of the magnetohydrodynamics equations, which brings about the fact that the solution ξ must be very small, $|\xi| << 1$, so that the non-linear terms can be neglected. This implies that $|\mathbf{b}_1|/|\mathbf{B}_0| < 1$. The error associated with this approximation is $\sigma \approx (|\mathbf{b}_1|/|\mathbf{B}_0|)^2$. The maximum possible value for the ratio $|\mathbf{b}_1|/|\mathbf{B}_0|$ is related to a clear statistical distinction between the maximum and the minimum value of the perturbed magnetic field, which is given approximately by $(|\mathbf{b}_1|/|\mathbf{B}_0|)/\sigma$ (in units of σ). To have a minimum 2σ distinction between the maximum and minimum magnetic field, we choose the maximum value of the perturbation such that $|\mathbf{b}_1|/|\mathbf{B}_0| \approx 0.5$.

The kind of conditions that we impose on the perturbation ξ due to the restrictions on ρ_1/ρ_0 and b_1/B_0 determine the amplitude of ξ but do not exclude one solution ξ in favor of another ξ. In this way, our calculations do not determine the set of possible frequencies out of the continua, but determine the kind of oscillations related to these perturbations, and the range of possible periods of the oscillations.

3.4 Range of frequencies

In this work we were interested in calculating the eigenfunctions of the Hain–Lüst equation via the continua determined by the functions $w^2 = w_A^2$ and $w^2 = w_S^2$. In the present case, we have for these functions $w_A^2 \approx w_S^2$, due to the fact that the magnetic pressure is negligibly small when compared to the gas pressure ($B_0^2 << \gamma p$). As w_A and w_S depend linearly on B, the magnetic profiles used were such that there is no value of r for which B is zero, because, if $w_A = 0$ or $w_S = 0$, this means that the continua extend until $w = 0$ and in this way all the oscillatory modes below the continua would be killed. Otherwise, it is very reasonable that the magnetic field is non-zero inside the Sun if we choose magnetic profiles which value in the convective zone is $\sim 10^5$ G.

For the magnetic profiles given by (9) and (10) we have possible solutions for $w > 4.40 \times 10^{-5}\,\mathrm{s}^{-1}$ or $w < 5.98 \times 10^{-6}$, which gives a period of $\tau < 1.65$ days or $\tau > 12.14$ days, respectively. For the magnetic profile given by (9) and (11) we have $w > 4.95 \times 10^{-4}\,\mathrm{s}^{-1}$ or $w < 5.32 \times 10^{-6}\,\mathrm{s}^{-1}$, which gives $\tau < 0.15$ days or $\tau > 13.7$ days, respectively. For the magnetic profile given by (12) we have $w > 6.28 \times 10^{-4}\,\mathrm{s}^{-1}$ or $w < 2.56 \times 10^{-6}\,\mathrm{s}^{-1}$, which gives $\tau < 0.11$ days or $\tau > 28.5$ days, respectively.

3.5 Magnetic moment

We are considering the standard solar electron number distribution which implies that $10^{-16}\,\mathrm{eV} \leq (2^{1/2}/2)G_\mathrm{F}N_e(r) \leq 10^{-12}\,\mathrm{eV}$. In order to find an appreciable spin–flavor neutrino conversion governed by the equations of motion (1), we have to allow the other two relevant quantities in these equations, namely $\Delta m/4E$ and $\mu_\nu|\mathbf{B}_\perp(r)|$, to be approximately of the same order of $(2^{1/2}/2)G_\mathrm{F}N_e(r)$. Assuming the magnetic fields given by (9) and (10), if we take $\mu_\nu \approx 10^{-11}\mu_\mathrm{B}$ (μ_B is the Bohr magneton), the quantity $\mu_\nu|\mathbf{B}_\perp(r)|$ varies from approximately $10^{-14}\,\mathrm{eV}$ in the central parts of the Sun to $10^{-15}\,\mathrm{eV}$ in the beginning of the convective zone and smaller values than $10^{-16}\,\mathrm{eV}$ in the solar surface, giving the order of magnitude needed for appreciable conversion. For the magnetic field given by (11) and (12) we used $\mu_\nu = 2 \times 10^{-12}\mu_\mathrm{B}$, which gives

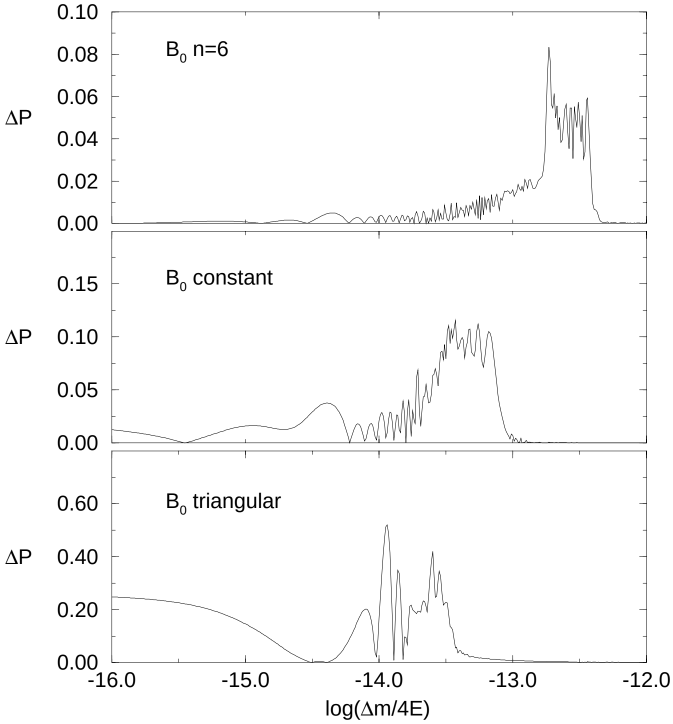

Fig. 2. Amplitude ΔP of the survival probability as a function of $\Delta m/4E$ for the magnetic profiles given by (9) and (10) (B_0 $n=6$), (12) (B_0 constant) and (9) and (11) (B_0 triangular)

$\mu_\nu|\mathbf{B}_\perp(r)|$ to be of the same order of $(2^{1/2}/2)G_{\mathrm{F}}N_e(r)$ in the convective zone.

4 Results

In the first row of Fig. 1 we present the profile of the radial displacement ξ_r, calculated by solving the Hain–Lüst equation (2), when the magnetic profiles are assumed to be given by (9), (10), (11) and (12), respectively, are assumed. It is important to notice that clearly different ξ_r wavelengths appear for each one of the magnetic fields employed. This will be reflected also in the MHD fluctuations of the matter density ρ_1/ρ_0 and the magnetic field b_1/B_0, which are directly calculated from ξ_r and are shown in the second and third rows of Fig. 1, respectively.

The Hain–Lüst solutions shown in Fig. 1 are found in the region of the MHD spectrum in which frequencies are smaller than the continuum frequencies: $\omega^2 < \omega_A^2 \approx \omega^S$. The period of the solutions found above the continua are smaller than $O(1\,\mathrm{s})$, very tiny, therefore, to be detected by present experiments.

In Fig. 2 we present the effects on the solar neutrino survival probability when the perturbations ρ_1 and b_1 are included in the evolution equations (1). In this figure we plot the difference of the survival probability calculated in two different situations: when the effect of the MHD perturbations maximally increases the survival probability and the opposite case when the perturbations destructively contribute to this probability, decreasing it.

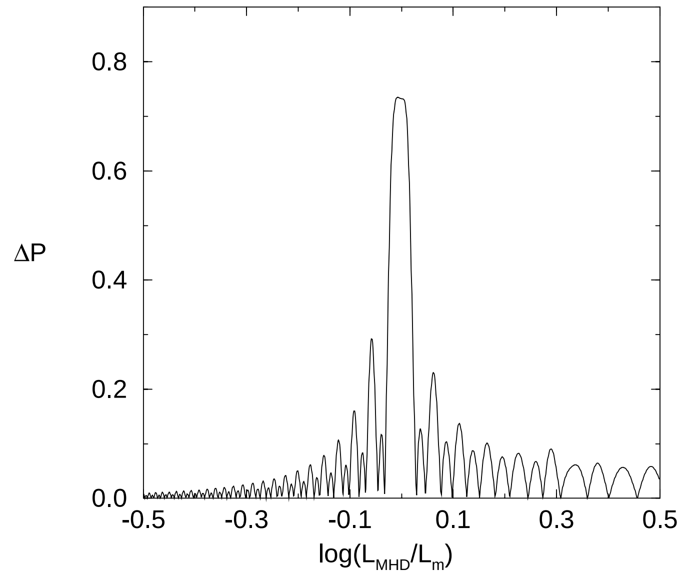

Fig. 3. The same survival probability difference as shown in Fig. 2, when a constant magnetic field is assumed, but varying the ratio between the perturbation wavelength and the neutrino oscillation length

We see that the range of the values of $\Delta m/4E$ for which this difference is significant varies for each of the magnetic field profile considered. This is a direct consequence of the appearance of a parametric resonance [13] in the evolution of the neutrino due to the MHD perturbations along its trajectory. To understand this effect we have to consider the neutrino oscillation length. When we have a neutrino oscillation length similar to the wavelength of the magnetohydrodynamic perturbations, a significant enhancement of the neutrino chirality conversion occurs. This is the parametric resonance which is clearly observed in the neutrino survival probability. In other words, when the neutrino is evolving, an intense chirality conversion from left- to right-handed neutrinos occurs when the magnetic field is increased by the perturbation. On the contrary, when the neutrino oscillation would lead to the opposite chirality conversion from right to left neutrino, this coincides with a period of lower magnetic field, and this conversion is suppressed. If the perturbation wavelength is very different from the neutrino oscillation length, then this effect will not be relevant and we can understand the behavior of Fig. 2 far from the peaks. Figure 3 illustrates this effect. Here we plot the same survival probability difference as presented in Fig. 2, when a constant magnetic field is assumed, but varying the ratio between the perturbation wavelength and the neutrino oscillation length.

If we compare the different MHD perturbations of Fig. 1 generated by the different magnetic field configurations, we see that they differ substantially in their typical wavelengths. We can associate the smaller wavelength (case (10)) with a parametric resonance in the lowest energy range of the neutrino, and the greatest oscillation length (case (11)) with the higher energy range. To present a more quantitative example, we can calculate the perturbation wavelength when using a particular magnetic field configuration. Let us consider the case (11) and compare with a typical corresponding neutrino oscillation length where the effect on the survival probability is significant. For this magnetic field configuration, we have an approximate perturbation wavelength of $7 \times 10^{-3} R_{\odot}$, or equivalently, $2 \times 10^{13}\,\mathrm{eV}^{-1}$. The range of a significant effect in the probability yields a neutrino oscillation length that lies in the range ~ 2–$6 \times 10^{13}\,\mathrm{eV}$. This makes evident the importance of the parametric resonance for the survival probability.

A final remark is in order. If we assume that the RSFP mechanism is the reason of the experimentally observed solar neutrino deficit, a typical magnitude of the parameter Δm is $O(10^{-7}$–$10^{-8})\,\mathrm{eV}^2$ [18]. Putting these numbers in the results shown in Fig. 2, we conclude that low energy neutrinos (0.1–1 MeV) will be more sensitive to parametric resonances. In this case, the kind of perturbations analyzed here could be tested by real time experiments that have a high efficiency for low energy neutrinos. This is the case for experiments like BOREXINO [23] and HELLAZ [24]. These should be able to look for variations of the detection rate for low energy neutrinos with periods of the order of some days, given the strong evidence for the interaction of the solar neutrinos with instabilities generated by the magnetohydrodynamics in the Sun.

Since MHD waves generate perturbations also on the matter density in the Sun, other neutrino conversion mechanisms that are sensitive to the matter density could be sensitive to the parametric effects analyzed in this paper. This is the case, for instance, for the MSW mechanism [25] and the neutrino conversion induced by flavor changing (FC) interactions [26]. In fact, parametric effects were explicitly analyzed in [27] and [28] in a phenomenological context. In these papers the authors concluded that the parametric effect in the MSW mechanism would be enhanced if the density fluctuations take place in the inner part of the Sun, near the resonances for adiabatic transitions. Since our perturbations are located in the convective zone, the parametric effects due to density fluctuations would not be very strong in the MSW context. Also, the fluctuations induced by MHD effects shown in Fig. 1 show very constrained matter density amplitudes. These are less than 1% except very close to the solar surface ($r/R_{\mathrm{Sun}} \approx 1$), where they achieve a maximum value of less than 2%. In fact, we obtain small parametric effects ($\Delta P \lesssim 10^{-4}$) due to the density perturbations in other neutrino conversion scenarios for the MHD waves obtained in this paper.

Time fluctuations are expected in several conversion mechanisms invoked in the solar neutrino context. The vacuum oscillation phenomenon [29,30] leads to seasonal fluctuations of the solar neutrino (beyond the standard geometrical factor) of which the period is one year. Day–night effects and the related seasonal variations are expected in the MSW [31] as well as in the FC scenario. Resonant spin–flavor precession generates a modulation of the neutrino flux due to the solar activity (period of eleven years) as well as some fluctuation of the neutrino flux when the Earth crosses the solar equator (period of half a year). Therefore, we believe that any periodic time fluctuation of the solar neutrino measurements of which the period does not coincide with the above mentioned ones can be taken as an indication of MHD modes in the sun. This would be evidence in favor of the resonant spin–flavor precession solution to the solar neutrino anomaly.

We conclude that maybe another effect has to be taken into account when we discuss possible solutions to the solar neutrino problem. In addition to the adiabatic parameter and the usual resonance effects, the interference between the oscillation length of the solar neutrinos and the solar perturbation wavelengths induced by MHD effects may lead to parametric resonances, playing an important role in the survival probability of solar neutrinos in the resonant spin–flavor precession scenario.

Acknowledgements. This work was supported by Fundação de Amparo à Pesquisa do Estado de São Paulo (FAPESP), Programa de Apoio a Núcleos de Excelência (PRONEX) and Conselho Nacional de Desenvolvimento Científico e Tecnológico (CNPq).

References

1. J. Bahcall, R. Ulrich, Rev. Mod. Phys. **60**, 297 (1988); J.N. Bahcall, Neutrino Astrophysics (Cambridge University Press, New York 1989); the neutrino fluxes as well as cross sections are available at URL http://www.sns.ias.edu/ jnb/
2. J.N. Bahcall, M.H. Pinsonneault, Rev. Mod. Phys. **67**, 781 (1995)
3. J.N. Bahcall, S. Basu, M.H. Pinsonneault, Phys. Lett. B **433**, 1 (1998)
4. For a recent review, see J. N. Bahcall in Neutrino '98, Proceedings of the XVIII International Conference on Neutrino Physics and Astrophysics, Takayama, Japan, 4–9 June 1998, edited by Y. Suzuki, Y. Totsuka, Nucl. Phys. B (Proc. Suppl.) (in press)
5. A. Cisneros, Astro. & Space Sci. **10**, 87 (1971); M.B. Voloshin, M.I. Vysotskii, L.B. Okun, Yad. Fiz. **44**, 677 (1986) [Sov. J. Nucl. Phys. 44 (1986) 440]; C.S. Lim, W.J. Marciano, Phys. Rev. D **37**, 1368 (1988); E.Kh. Akhmedov, Phys. Lett. B **213**, 64 (1988); A.B. Balantekin, P.J. Hatchell, F. Loreti, Phys. Rev. D **41**, 3583 (1990); J. Pulido, Phys. Rep. **211**, 167 (1992); E.Kh. Akhmedov, A. Lanza, S.T. Petcov, Phys. Lett. B **303**, 85 (1993); P.I. Krastev, Phys. Lett. B **303**, 75 (1993)
6. K. Lande (Homestake Collaboration) in Neutrino '98 [4]
7. Y. Fukuda et al. (Kamiokande Collaboration), Phys. Rev. Lett. **77**, 1683 (1996)
8. V. Gavrin (SAGE Collaboration) in Neutrino '98 [4]
9. T. Kirsten (GALLEX Collaboration) in Neutrino '98 [4]
10. Y. Suzuki (SuperKamiokande Collaboration) in Neutrino '98 [4]
11. M.M. Guzzo, N. Reggiani, J.H. Colonia, Phys. Rev. D **56**, 588 (1997)

12. M.M. Guzzo, N. Reggiani, J.H. Colonia, P.C. de Holanda, Effects of magnetohydrodynamics matter density fluctuations on the solar neutrino resonant spin–flavor precession, hep-ph/9812390
13. V.K. Ermilova, V.A. Tsarev, V.A. Chechin, Kr. Soob, Fiz., Lebedev Inst. **5**, 26 (1986); E. Akhmedov, Yad. Fiz. **47**, 475 (1988); P.I. Krastev, A.Yu. Smirnov, Phys. Lett. B **226**, 341 (1989)
14. E.R. Priest, Solar Magnetohydrodynamics (D. Reidel Publishing Company 1987)
15. I.B. Bernstein, E.A. Frieman, M.D. Kruskal, R.M. Kulsrud, Proceedings Roy. Soc. A **224**, 1 (1958)
16. J.P. Goedbloed, Physica **53**, 412 (1971); J.P. Goedbloed, P.H. Sakanaka, The Physics of Fluids **17**, 908 (1974)
17. E.Kh. Akhmedov, A. Lanza, S.T. Petcov, Phys. Lett. B **303**, 85 (1993)
18. M.M. Guzzo, H. Nunokawa, Current status of the resonant spin–flavor solution to the solar neutrino problem, hep-ph/9810408
19. H. Minakata, H. Nunokawa, Phys. Rev. Lett. **63**, 121 (1989); A.B. Balantekin, P.J. Hatchell, F. Loreti, Phys. Rev. D **41**, 3583 (1990); H. Nunokawa, H. Minakata, Phys. Lett. B **314**, 371 (1993)
20. H. Nunokawa, A. Rossi, V.B. Semikoz, J.W.F. Valle, Nucl. Phys. B **472**, 495 (1996)
21. S. Turck-Chiéze et al., Phys. Rep. **230**, 57 (1993)
22. G. Fiorentini, B. Ricci, Solar neutrinos: where we are and what is next? astro-ph/9801185
23. S. Malvezzi, Nucl. Phys. B (Proc. Suppl.) **66**, 346 (1998)
24. T. Patzak, Nucl. Phys. B (Proc. Suppl.) **66**, 350 (1998)
25. S.P. Mikheyev, A.Yu. Smirnov, Sov. J. Nucl. Phys. **42**, 913 (1985); L. Wolfenstein, Phys. Rev. D **17**, 2369 (1978)
26. M.M. Guzzo, A. Masiero, S.T. Petcov, Phys. Lett. B **260**, 154 (1991); E. Roulet, Phys. Rev. D **44**, 1692 (1991)
27. E.Kh. Akhmedov, Sov. J. Nucl. Phys. **47**, 301 (1988)
28. P.I. Krastev, A.Yu. Smirnov, Phys. Lett. B **226**, 341 (1989)
29. M. Maris, S.T. Petcov, SISSA 13/99/EP, hep-ph/9903303
30. V. Barger, K. Whisnant, hep-ph/9903262
31. P.C.de Holanda, C. Peña-Garay, M.C. Gonzalez-Garcia, J.W.F. Valle, hep-ph/9903473